Effects of Acoustic Disturbances on Measured Flow Characteristics Through a Contraction

J. Tan-atichat* and S. Harandi†
State University of New York, Buffalo, New York

An experiment involving the addition of randomly phased broadband acoustic disturbance to the flow through an axisymmetric contraction was conducted. Measurements of flow characteristics such as turbulence intensities, velocity spectra, and coherence functions were made at various locations through the contraction using two flow conditions. Acoustic excitation was shown to substantially increase the measured streamwise component of turbulence while leaving the radial component virtually unchanged. Although the radial component of turbulence energy remains relatively unaffected (less than 3%) inside the contracting region, a sudden increase was observed at the downstream end of the contraction. The coherence at $x/L = 0.75$ for the acoustically excited flow contains a small band of frequencies with low coherence. The location of the low-coherence frequency band was sensitive to the incoming flow condition, suggesting some type of turbulence/acoustic interaction.

Nomenclature

A = area
c = contraction area ratio
f = frequency, Hz or kHz
L = contraction length
M = turbulence-generating grid mesh size
r = radial coordinate, measured from centerline
R, $R(x)$ = radius of contraction contour at x
s = lateral distance from the axis of symmetry
SPL = sound pressure level (dB Re 2×10^{-5} N/m^2)
u' = root-mean-square of velocity fluctuations in the streamwise direction
U, $U(x)$ = streamwise mean velocity
v' = root-mean-square of velocity fluctuations in the radial direction
V = radial (or lateral) component of mean velocity
x = direction parallel to test section and contraction's axis of symmetry

Subscripts
a = value for acoustically excited condition
e = value at exit of contraction
i = value at inlet to contraction

Introduction

CONTRACTIONS are used extensively as flow management devices to tailor mean and turbulence characteristics in a variety of flow facilities. Investigators such as Tsien,[1] Batchelor and Shaw,[2] Smith and Wang,[3] Thwaites,[4] Jordinson,[5] Cohen and Ritchie,[6] Bradshaw and Pankhurst,[7] Gay et al.,[8] Chmielewski,[9] Morel,[10,11] Nagib et al.,[12] have studied ways of improving the design of a contraction to reduce the relative turbulence and the boundary-layer thickness, to tailor turbulence characteristics, and/or to improve mean velocity uniformity in wind tunnels. Mild contractions were also used to obtain isotropic turbulence in order to improve the validity of comparisons between experiments and theories that assume an isotropic turbulence behavior (Refs. 13 and 14). Over the past few decades, numerous researchers have focused on the effect of contractions on grid-generated turbulence. Such flow characteristics may profoundly affect the results of certain experiments dealing with the transition of laminar boundary layers to turbulence. Design parameters such as contraction shape and contraction ratio have been investigated by Uberoi[15] and by Ramjee and Hussain.[17] More recently, Tan-atichat[18] suggested that the incoming turbulence characteristics just upstream of the contraction are parameters of utmost importance in determining the effectiveness of turbulence reduction through it. Operationally, a contraction can be viewed as a turbulence manipulator in a manner analogous to the way that Loehrke and Nagib[19] view honeycombs, screens and perforated plates; i.e., it acts on the incoming flow and turbulence, suppressing and altering the flow's characteristics, then "produces" mean flow and turbulence characteristics at the downstream end which depend (nonlinearly) on the characteristic parameters of the contraction as well as the incoming flowfield. When acoustic energy is present in the flow, it can be viewed as an additional parameter needed to characterize the incoming flowfield. Although previous investigations have focused on turbulence characteristics through contractions (e.g., Refs. 12–24), none have included a study of turbulence characteristics in the presence of significant acoustic excitation.

Most wind tunnels have varying amounts of residual acoustic energy that depend to a large extent on the method used to provide air motion inside the wind tunnel. A major source of acoustic noise can be traced to blowers, fans, or valve noise from a compressed-air or vacuum supply. Unless extraordinary measures (e.g., see Kadman and Hayden[25]) are taken to reduce its intensity, a large percentage of these acoustic disturbances can propagate through the settling chamber, the contraction section, and on to the test section. Although there have been numerous studies on fan noise control and duct acoustics (e.g., Refs. 26 and 27), few studies have focused on the effects of acoustic disturbances on turbulence characteristics through a contraction. When present at sufficiently high levels, its effects on the measured characteristics of the fluctuating velocity components need to be understood. This is especially important in the design of high-performance contractions for very low-turbulence wind tunnels that are intended for transition or laminar flow control studies.

Received Feb. 15, 1986; presented as Paper 86-0766 at the AIAA 14th Aerodynamic Testing Conference, West Palm Beach, FL, March 5-7, 1986; revision received Aug. 11, 1986.

*Assistant Professor, Mechanical and Aerospace Engineering. Member AIAA.
†Graduate Student.

Experimental Apparatus and Approach

Experimental Facility

The present investigation was conducted in an open-return wind tunnel shown in Fig. 1. Acoustic excitation is introduced by a 16.5-cm loudspeaker (speaker resonant frequency ≈ 45 Hz) mounted on a conical "horn" at one end of the wind tunnel. Downstream of the 42-cm conical section, airflow is introduced into the wind tunnel by means of a centrifugal blower connected to the settling chamber at a 45-deg angle via a 15.5-cm-diam duct. For this experiment, the blower speed was adjusted to 1400 rpm by a Variac. Airflow and acoustic waves pass through a matrix of 25-cm-long plastic drinking straws (i.e., honeycomb) held in place at the downstream end by a 0.084-cm mesh screen (solidity of 0.33). The 29.2-cm-i.d. settling chamber is made up of carefully joined plexiglas sections. A perforated grid was inserted to produce a different turbulence flow condition upstream of the contraction. This grid, identical to PP3 in Tan-atichat et al.,[28] was manufactured from 1.6-mm-thick punched steel plates. The 6.35-mm-diam holes are arranged in a hexagonal array with a mesh size M of 0.80 cm and a solidity of 0.42. A 35.3-cm space ($x/M = 44$) between the grid and the contraction inlet allows the turbulence generated by the grid to attain homogeneity and approximate isotropy. The flow is then accelerated through an axisymmetric matched-cubic contraction with an area ratio of 14 : 1. The contracting section is 40 cm long with a 7.8-cm-diam exit. A 5-cm length of constant-diameter duct is located downstream of the contraction exit. Thus, measurements pertaining to the exit section were not made in a freejet environment to avoid the influence of entrainment. The length-to-inlet diameter ratio (L/D) of the contraction is 1.37, with the inflection point located at $x/L = 0.6$. This contraction was designed using the method described by Morel[10] to avoid flow separation near the inlet. Flow velocity at the contraction's inlet and exit was 1.3 and 20.5 m/s, respectively. The boundary layer at the exit was turbulent. Reynolds number based on the exit diameter was 1.08×10^5

Instrumentation

White noise from an Elgenco Gaussian noise generator was amplified by a Wilcoxon Research Model PA7B 125-W power amplifier that powered the 16.5-cm loudspeaker when acoustic excitation was used. Sound pressure level measurements were made with a Brüel and Kjaer (B&K) Type 4165 one-half-in. condenser microphone connected to a B&K Type 2209 Impulse Precision Sound Level Meter. This microphone, when used in conjunction with the B&K Type 2619 preamplifier, is capable of an essentially flat (± 2 dB) response from 4 Hz–20 kHz. The microphone/sound level meter combination was calibrated with a B&K Type 1562A Sound Level Calibrator. Flat frequency response weighting was used. Frequency spectra of the acoustic excitation were measured with a Nicolet Model 660A FFT analyzer (bandwidth of 50 Hz for an analysis range of 20 kHz).

Velocity measurements were made with three hot-wire probes, namely, two single-sensor probes, and one cross-wire probe, all with an active sensor length of 1 mm. The 5-μ tungsten hot wires were calibrated in a low-turbulence calibration facility built by Woo.[29] The hot wires were operated in a constant temperature mode at an overheat ratio of 1.7 using DISA Models 55M01 anemometers and 55M25 linearizers.

Conversion of the cross-wire probe signals to the streamwise and radial (or lateral) velocity components was done by the traditional sum-and-difference technique with a DISA Model 52B25 Turbulence Processor, assuming a cosine law angular response. Because flow angles with respect to the probe axis were small and turbulence intensities low, use of the cosine law relation is justified for the present study. The Nicolet Model 660A FFT analyzer was used to compute velocity spectra and coherence functions. Results were plotted with an X-Y plotter. Since most of the turbulence and acoustic excitation energy of interest occurred in the low-frequency range, the analysis range was set to 1 kHz. This gave a frequency resolution of 2.5 Hz.

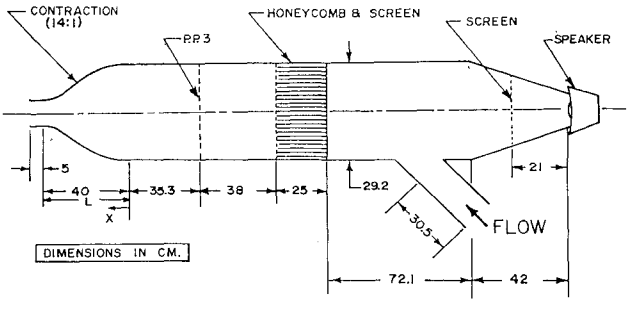

Fig. 1 Schematic of test facility.

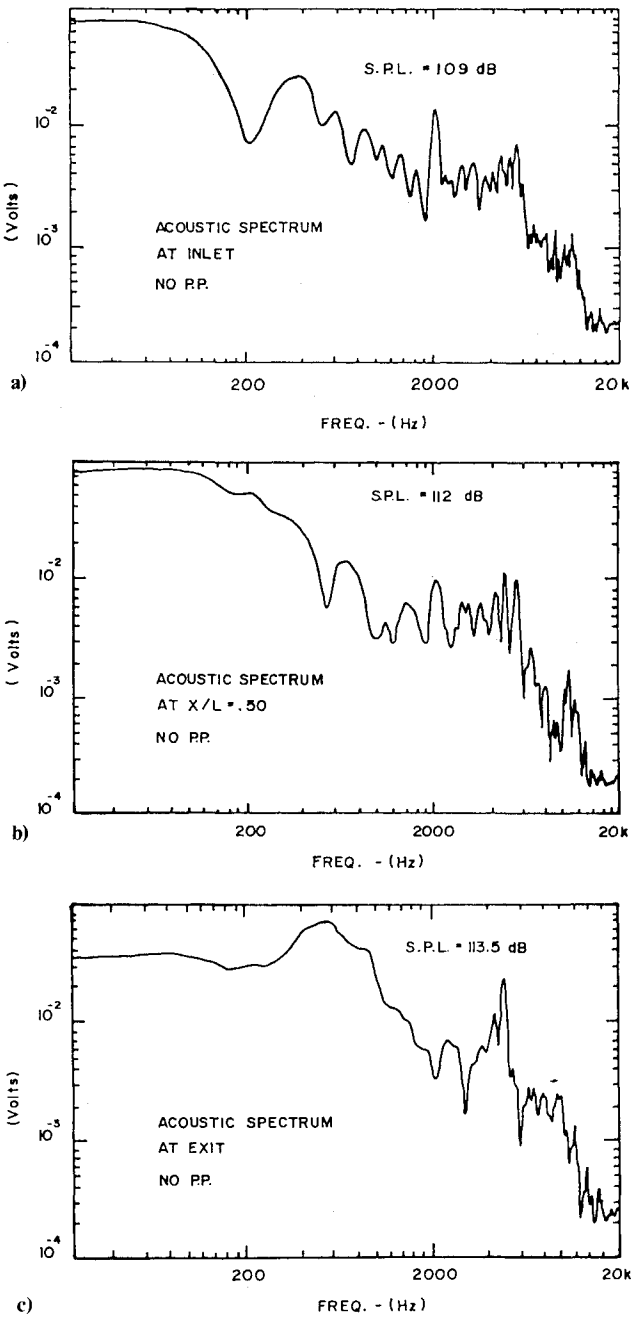

Fig. 2 Acoustic spectrum at a) inlet, b) $x/L = 0.5$, and c) exit of the contraction.

Experimental Approach

Randomly phased broadband noise was selected as the acoustic source instead of single-tone excitation for several reasons. First, it allows the system's response to an entire band of excitation frequencies of interest to be analyzed at once. Second, it reduces the problem of setting up very large amplitude standing waves at various characteristic frequencies of the experimental apparatus because of high input energy concentration at the excitation frequency for a single-tone source. All of the system's characteristic frequencies are identified at once so that there will be less of a chance of missing some of them. However, because all characteristic frequencies are simultaneously excited, it is more likely to produce very complicated spectra, making analysis more difficult. Notwithstanding this difficulty, a strong motivation for using broadband excitation is that the noise spectrum emitted by high-speed flow passing control valves in compressed-air and vacuum-driven wind tunnels resembles this type of acoustic source.

Acoustic spectral measurements were made with the microphone placed on the axis of symmetry inside the contracting section facing directly upstream with no flow. The output from the B&K sound level meter preamplifier and equalization circuits was fed into the FFT analyzer to obtain the acoustic excitation spectra at various axial positions inside the contraction.

Two general schemes were used to acquire turbulence and mean velocity data. The first procedure used two single-sensor probes that sense only the u' velocity fluctuations. Both probes were placed in the contraction section such that their sensing elements (i.e., the wires) were horizontal. Throughout this experiment, both sensors were moved in unison in the axial direction, keeping the streamwise position of the sensors identical. One of the sensors was placed on, and was moved only axially along, the contraction's axis of symmetry, while the other (vertically offset) sensor could also be traversed along the radial direction (vertical for the present experiment). The two sensors were kept parallel to each other. This arrangement maximized the spatial resolution in the radial direction (i.e., the vertical direction for the present arrangement). At each axial position, data were collected at sensor separation distances of 1, 2, and 3 cm. Four axial locations, namely $x = 0$ (contraction inlet), $x = 20$, 30, and 40 cm (contraction exit) were used. Ideally, it is advantageous to use cross-wires for each probe so that both the streamwise and the radial components of turbulence and their cross statistics could be measured. Cross-wires were not used here because of the unavailability of additional signal processing instrumentation. However, the present arrangement still enabled measurements to be made of the streamwise component of cross-correlation and coherence functions at various separation distances as well as the streamwise mean velocity and turbulence intensity at different radial positions.

A second procedure was used to survey both the streamwise and the radial components of turbulence characteristics through the contraction with a single cross-wire probe. For this part of the experiment, the X probe was located on the contraction's centerline and traversed axially to acquire data at five locations.

Two test flow conditions were used. The first test flow condition was obtained without the P.P.3 perforated plate shown in Fig. 1. This flow condition ($u' = 6.6\%$) will be referred to as flow condition T1. The second test condition, T2, was generated with the perforated plate present. This resulted in a homogeneous and approximately isotropic turbulence condition with a streamwise turbulence intensity of 4.6% at the contraction inlet.

Data were acquired with and without the imposed 109-dB SPL broadband acoustic excitation. Statistical results were averaged over 128 ensembles by the FFT analyzer. In most plots, the streamwise and lateral components of velocity fluctuations or turbulence energy were normalized by their respective values at the contraction inlet.

Results and Discussion

Note that the origin for the streamwise position is located at the contraction inlet and that the length and location of the contracting section is shown as the dimension L when results are plotted against downstream distance.

Acoustic Measurements

The acoustic excitation spectrum used in the present investigation was measured at three axial positions along the centerline of the contraction both with and without the P.P.3 grid. Only the spectra obtained without the turbulence-generating grid are shown because the presence of P.P.3 did not appear to affect the acoustic spectra. Up to 20 kHz, this grid can be considered acoustically transparent. This is not surprising because similar grids have been routinely used for grilles in high-fidelity speaker systems.

The overall sound pressure level at the contraction inlet was 109 dB SPL. The acoustic spectra in Fig. 2 show that a large percentage of this broadband excitation energy is below 1 kHz. This is also the frequency range where energy-containing turbulent fluctuations are located. Close examination shows that a significant shift of energy from the low frequencies to higher ones (approximately 300–800 Hz) occurred as the microphone was traversed from inlet to exit. An increase of 4.5 dB in the overall SPL was also noted. The contraction, acting as an "acoustic duct," can amplify the sound pressure level significantly because of its geometry.

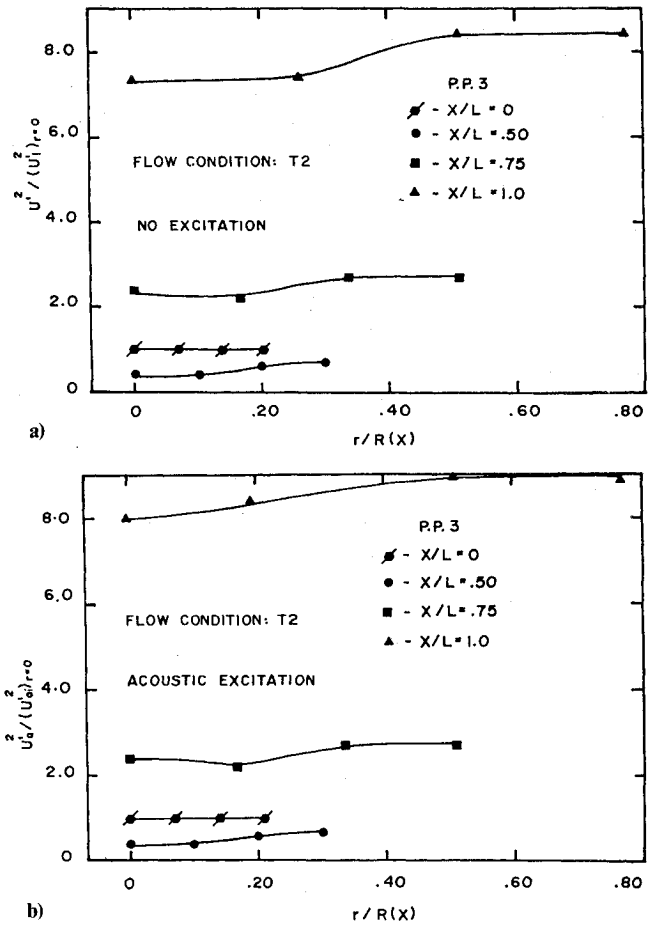

Fig. 3 Radial distribution of the normalized streamwise component of turbulence energy at various axial positions in the contraction using flow condition T2 a) without and b) with acoustic excitation.

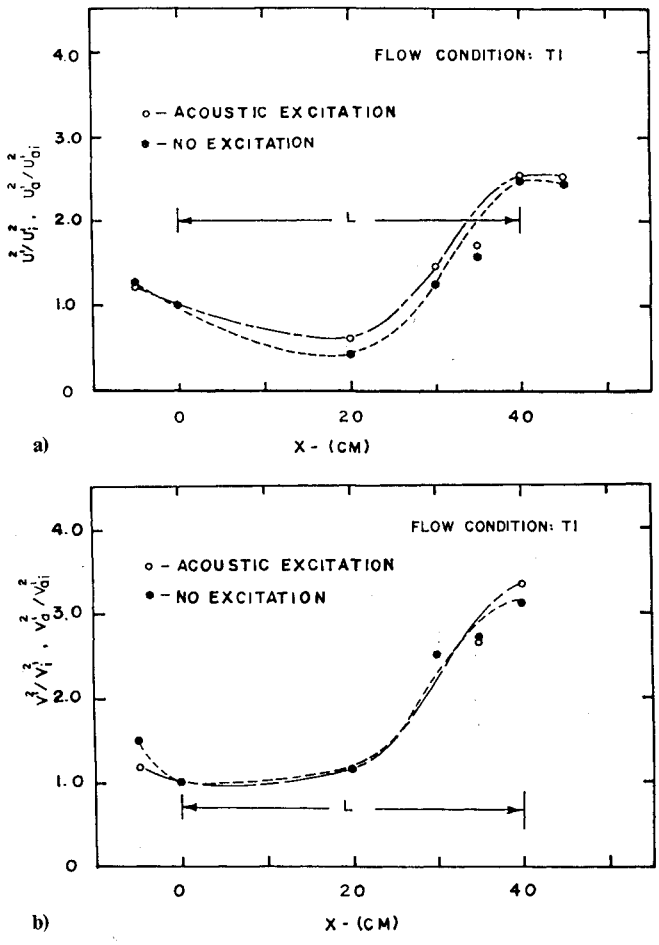

Fig. 4 Normalized turbulence energy through contraction along axis of symmetry with and without acoustic excitation for the a) streamwise and b) radial component.

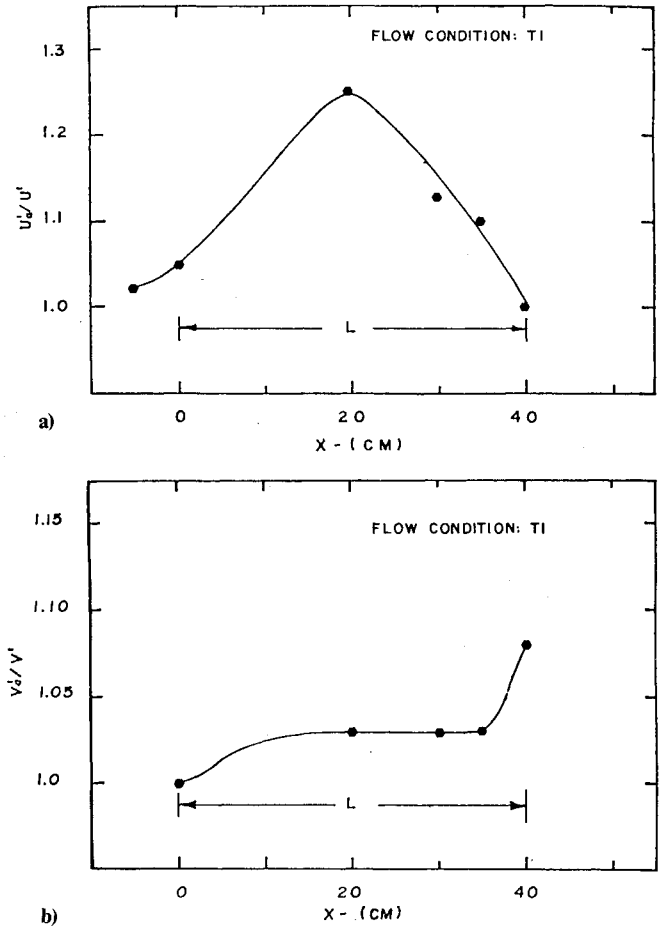

Fig. 5 Ratio of acoustically excited to unexcited velocity fluctuations along the centerline through the contraction using flow condition T1: a) streamwise component; b) radial component.

Radial Variation of Turbulence Energy

Figure 3 shows the streamwise component of turbulence energy through the contraction as a function of radial position. The radial distances were normalized by the local radius of the contraction contour. The results clearly indicate that, downstream of the inlet section, turbulence energy increases slightly as the distance from the centerline is increased. However, the effect is not significant until the middle of the contraction is reached. Analysis by Hultgren and Chen[30] predicts a slight decrease in the streamwise turbulence kinetic energy with radial position instead of the slight increase found experimentally. A comparison of Fig. 3a with Fig. 3b seems to indicate that at the contraction exit, when acoustic excitation is present, the increase in the streamwise turbulence energy with radial distance from the axis of symmetry occurs sooner than it did for the unexcited case.

Axial Variation of Turbulence Energy

The axial development of both the streamwise and the radial components of turbulence energy along the centerline through the contracting section for flow condition T1 is shown in Fig. 4. These results are consistent with those obtained by Uberoi,[15] Ramjee and Hussain,[17] and Tan-atichat.[18] The streamwise component of turbulence energy (shown in Fig. 4a) decreases initially as the flow begins to go through the contraction. It reaches a minimum at $x/L = 0.5$, then increases toward the exit. This is in contrast to the rapid distortion theory (Batchelor and Proudman[31]) which predicts a monotonic decrease of the streamwise energy component through the contraction since the contraction area is continually decreasing. The discrepancy between theory and experiment could result from several factors, such as 1) the theory's assumptions of very small turbulence scales in comparison with the contraction's characteristic length scale, and 2) the theory's neglect of viscous dissipation and nonlinear effects: all of which are violated to some degree in an actual flow. Recently, Tsugé[24] was able to obtain good qualitative agreement between the theory and experiments by taking the effects of large turbulent eddies into account. The radial component of turbulence energy shown in Fig. 4b behaved qualitatively as predicted by classical theory (Ref. 31), that is, it increased through the contraction. However, the magnitude of increase was less than theoretically predicted. A first-order correction to account for viscous decay was suggested and applied by Tan-atichat[18] with some success to improve the correlation between predicted and observed behavior for turbulent flows through contractions. For this 14:1 contraction with flow condition T1, the total turbulence kinetic energy at the exit of the contraction is more than three times larger than its value at the inlet section, most of it contained in the radial component.

At each of the axial locations downstream of the contraction inlet, the streamwise turbulence energy in the acoustically excited flow is seen to have a higher value than the corresponding unexcited flow. The difference diminishes at and beyond the exit of the contraction. This observation suggests that the presence of the acoustic energy contributes more to the measured turbulence energy in a rapidly contracting region. Figure 4b reveals that, with the exception of the contraction's exit, acoustic excitation effects are much smaller on the radial turbulence energy. A better comparison can be made by plotting the ratio of the turbulent velocity fluctuations in an

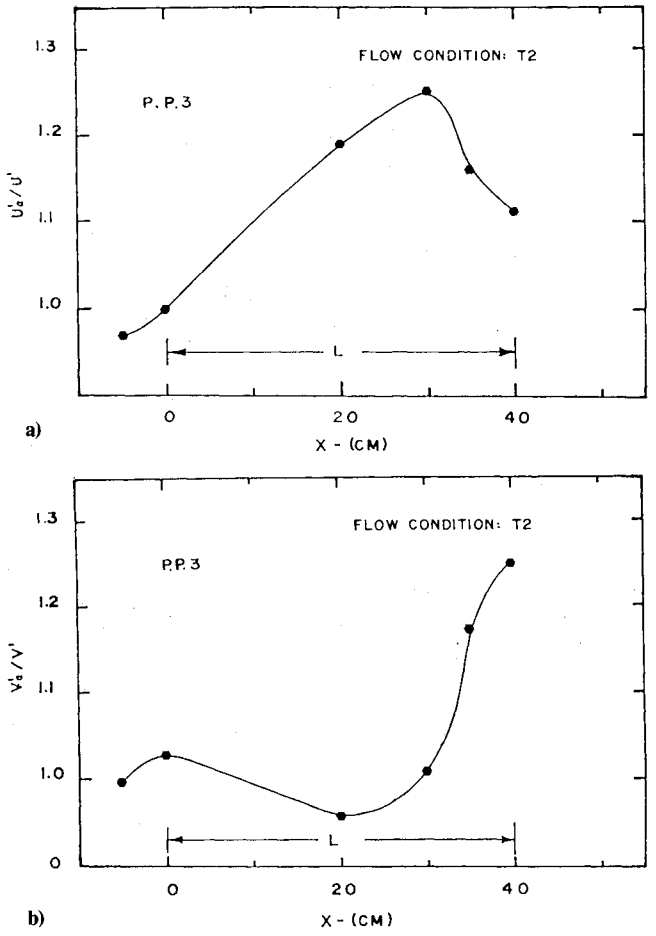

Fig. 6 Ratio of acoustically excited to unexcited velocity fluctuations along the centerline through the contraction using flow condition T2: a) streamwise component; b) radial component.

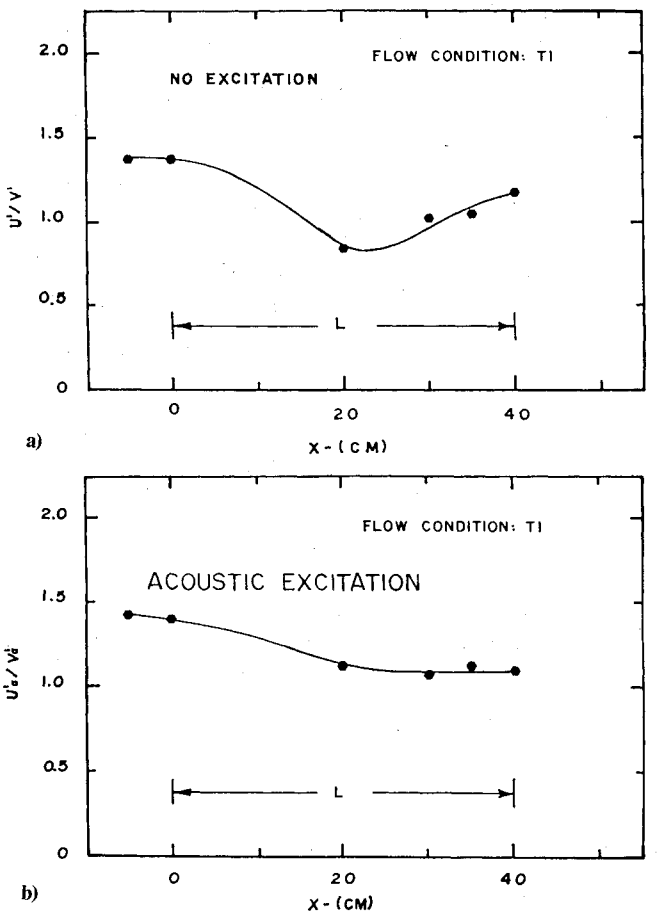

Fig. 7 Turbulence isotropy along contraction's centerline using flow condition T1 a) without and b) with acoustic excitation.

acoustically excited flow to those in an unexcited flow vs the distance through the contraction for the streamwise (Fig. 5a) and the radial (Fig. 5b) components. Focusing on the streamwise component, a maximum increase of about 25% is seen to occur at $x/L = 0.5$ where the local contraction ratio c was 2.2. Several possible reasons for this behavior are explored. It has been suggested that an acoustically induced flow separation bubble within the nozzle could account for this u' increase within the contraction. However, the design of this nozzle is such that flow separation in the absence of acoustic excitation is very unlikely[10] since the design pressure coefficient at the inlet is not close to the value at incipient separation. If an acoustically induced separation is indeed the culprit, this acoustic disturbance must have a very strong destabilizing effect on the boundary layer to cause such a separation, especially in a contracting stream. Flow fluctuations induced by the acoustic excitation and reflected from the contraction boundary are another possible (and more likely) cause. Since measurements were made along the contraction's centerline, axial symmetry also explains the relatively small effect (less than 3%) on the radial component except at the exit. Qualitatively, results using flow condition T2 (Fig. 6) show somewhat similar behavior. However, in contrast to the T1 condition, the peak u'_a/u' occurs farther into the contraction, and the effect of acoustic excitation on the measured velocity fluctuations is still quite significant at the contraction exit. This result seems to suggest that turbulence in the flow interacts with the acoustic field. Depending on the incoming turbulence characteristics, acoustic/turbulence interactions can produce different results inside and downstream of the contraction. Further evidence will be presented in a later section.

In general, for turbulent flows through axisymmetric contractions, u' will decrease relative to v' for mild contractions ($c \leq 4$), or the increase in u' toward the contraction exit will be smaller than that of v' for moderate ($6 \leq c \leq 12$) to high ($c \geq 16$) contraction ratios. The degree of turbulence isotropy as indicated by the u'/v' ratio will show a significant variation through the contraction. Specific details of this variation through the contraction will depend to a large extent on the turbulence scale upstream of the contraction as well as on the contraction geometry.[18,24] Figure 7 shows anisotropy of the velocity fluctuations through the contraction. The result in Fig. 7a for the unexcited flow is typical of those obtained for upstream turbulence with relatively small integral scales. Because acoustic excitation increases the measured streamwise component of velocity fluctuations more than the radial component, its presence will distort the u'/v' plot and tends to show a more uniform, i.e., less contorted behavior through a contraction. Similar results were also obtained with flow condition T2.

Spectral Measurements

These results were obtained with an X probe placed on and traversed along the centerline of the contracting section. Velocity spectra obtained from T1 are shown in Figs. 8–10. These are arranged to show the spectra from the inlet ($x/L = 0$) to the exit ($x/L = 1$). At each axial position, spectral plots of streamwise and radial velocity fluctuations are shown first without, then with, acoustic excitation.

A number of narrow-band peaks can be seen in all the velocity spectra. These frequency peaks were traced to several nonturbulence-related sources. The peak just above 500 Hz is the fundamental blade-passing frequency of the blower. The

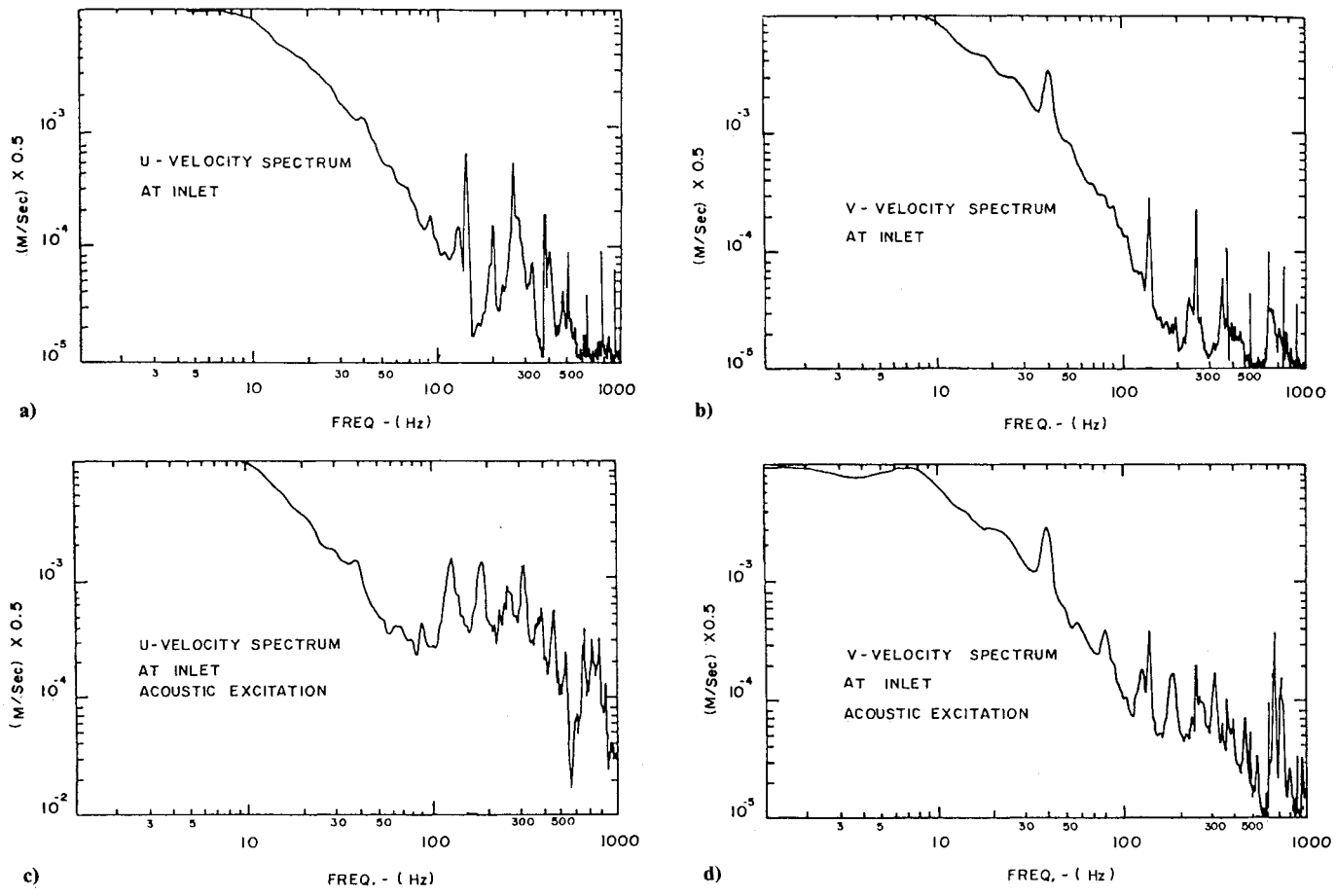

Fig. 8 Turbulence velocity spectra at contraction inlet. No acoustic excitation: a) streamwise component; b) radial component. With acoustic excitation: c) streamwise component; d) radial component.

quarter-wave "pipe organ" resonance of the facility was estimated to be approximately 33 Hz. Speaker resonance frequency is about 42–45 Hz. Other narrow band peaks are caused by harmonics of the 60 Hz ac power source. These peaks should be ignored whenever they are irrelevant to the assessment or interpretation of the results. Instead, the reader should concentrate on the change in the general shape of these spectra at the different positions and for different conditions.

Both the streamwise and radial components of turbulence energy are augmented as the flow traverses through the contraction, even without the imposed acoustic excitation. Harandi[32] noted that at each given axial position, no significant difference was detected in the streamwise velocity spectra at different radial positions. Exciting the flow acoustically, the measured turbulence energy is shown to increase as expected. Consistent with the results presented earlier, comparisons made between Figs. 8a and 8b with Figs. 8c and 8d show that the increased level of turbulence energy caused by acoustic excitation is much larger for the streamwise than for the radial component. This observation holds throughout the contracting section from inlet to exit (see Figs. 9 and 10 also). Similar results were also obtained with flow condition T2.

A very interesting result is shown at $x/L = 0.75$, whereby the acoustically excited u' spectrum exhibits a minimum at a frequency between 400–500 Hz. This phenomenon is probably the net effect of the interaction between the turbulence and acoustic reflections from the contraction boundary. Using the reflecting plane theory, calculations of the noise level in a combustor by Huff[33] show that fluctuating pressure spectra behaved in a similar manner when relatively high reflection factors were assumed. Results obtained with turbulence flow condition T2 revealed the same findings.

Coherence Measurements

Coherence functions for two single-sensor probes separated at various radial distances were recorded for both flow conditions at different axial positions. Generally speaking, the coherence function can be interpreted as the fractional portion of the mean square value of the velocity fluctuations measured by one probe that is directly (and uniquely) related to the ones measured by the other probe at frequency f. If the velocity fluctuations sensed by the two probes (separated spatially) are uniquely related at all frequencies, then the coherence function will be unity for all frequencies. However, if the fluctuations are completely unrelated, then the coherence function is zero.

In a truly homogeneous isotropic turbulent flow without acoustic excitation, one would expect zero coherence between the two probes whenever the separation distance is greater than about twice the integral length scale of the energetic turbulent eddies. However, the experimental results show a small amount of nonzero broadband coherence in both test flow conditions at the contraction's inlet. This is likely to result from the residual pressure-induced streamwise velocity fluctuations caused by the blower.

The narrow-band peaks that were present in the velocity spectra show up prominently in these coherence diagrams. As discussed in the previous section, these are caused by the blower's blade-passing frequency, the Helmholtz and pipe organ resonator frequencies of the system, speaker resonance, and power line harmonics. The reader should not allow the presence of these peaks to mask the assessment of acoustic excitation effects on turbulence through the contraction.

Coherence is higher downstream of the contraction (without the imposed acoustic excitation) because residual blower-

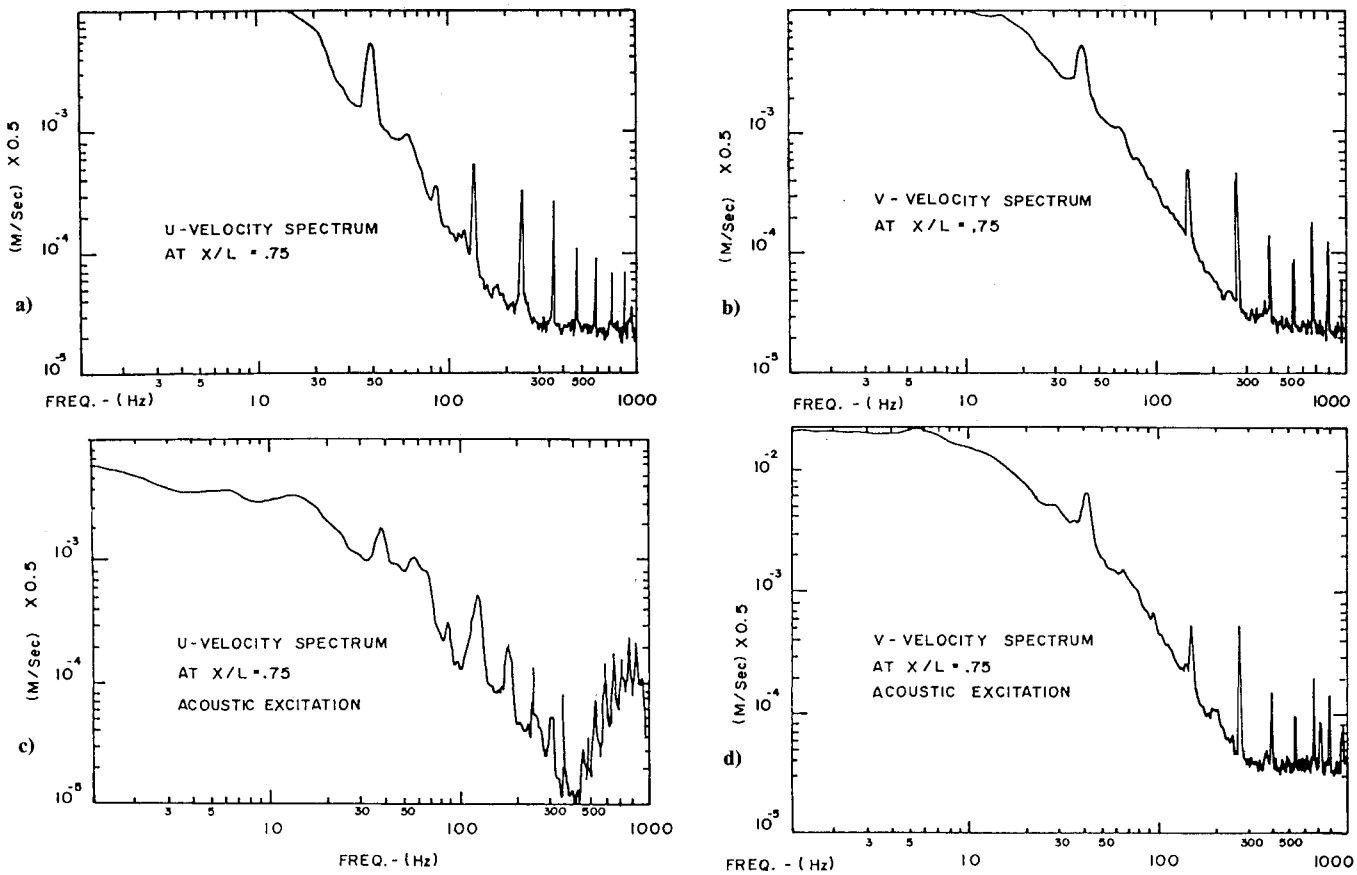

Fig. 9 Turbulence velocity spectra at contraction $x/L = 0.75$. No acoustic excitation: a) streamwise component; b) radial component. With acoustic excitation: c) streamwise component; d) radial component.

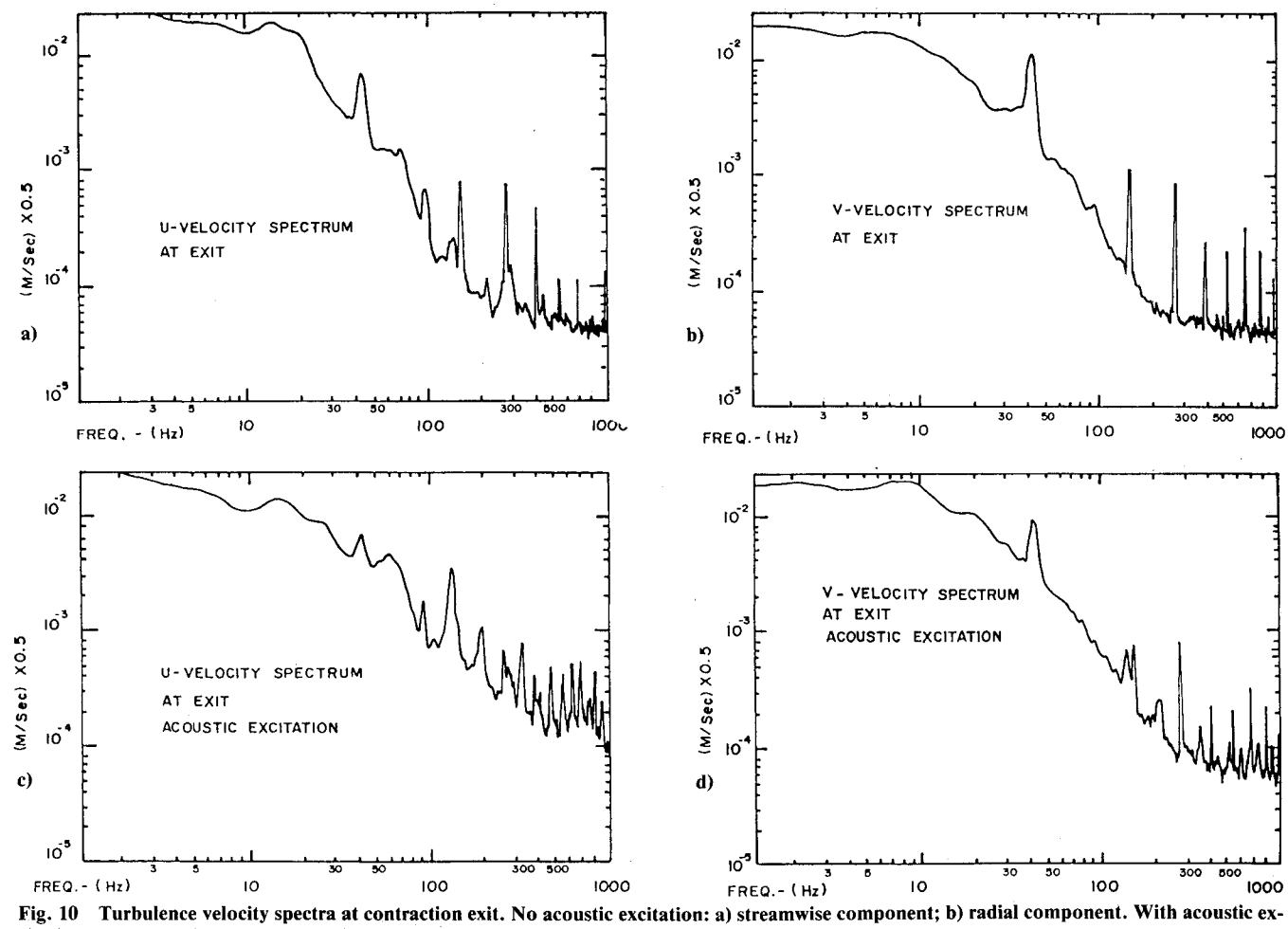

Fig. 10 Turbulence velocity spectra at contraction exit. No acoustic excitation: a) streamwise component; b) radial component. With acoustic excitation: c) streamwise component; d) radial component.

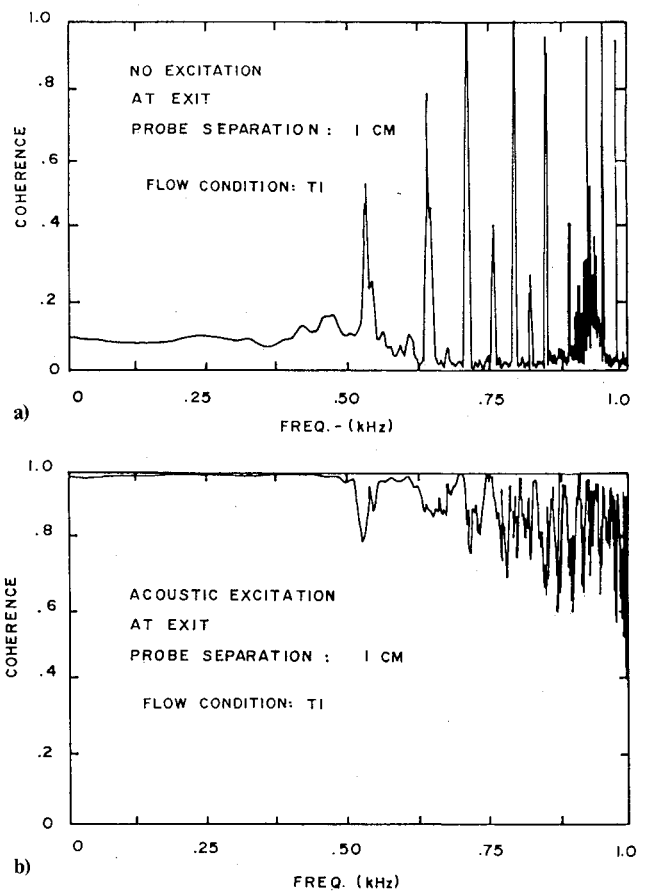

Fig. 11 Coherence function of streamwise velocity at contraction exit between two probes separated radially (1-cm probe separation: $r/R(x) = 0.26$) using flow condition T1: a) no acoustic excitation; b) with acoustic excitation.

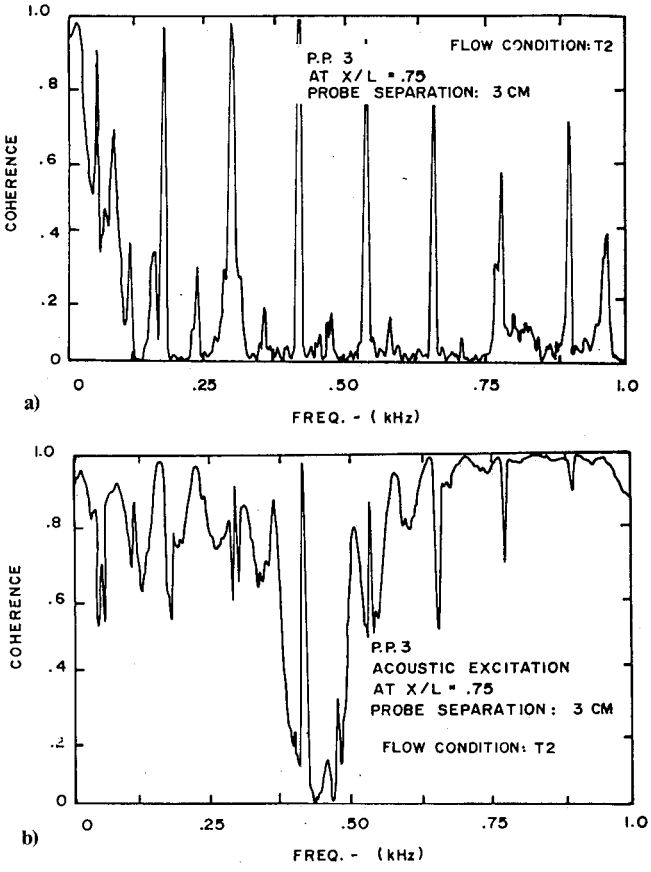

Fig. 12 Coherence function of streamwise velocity at $x/L = 0.75$ between two probes separated radially (3-cm probe separation: $r/R(x) = 0.51$) using flow condition T2: a) no acoustic excitation; b) with acoustic excitation.

induced u' velocity fluctuations are amplified through the contracting section by virtue of its geometry and mass continuity. When the T2 flow condition was used, coherence was detected over a narrower range of frequencies, depending on the probes' separation. Outside this range the coherence is essentially zero, with the exception of the narrow-band peaks mentioned. Compared to T1, the more spatially random u' velocity fluctuations in the T2 flow condition tend to reduce the effect of residual blower-induced coherent u'-like fluctuations. (Note that acoustically induced u'-like fluctuations are not random in the radial direction.) Figure 11 shows that acoustically exciting the flow produces an almost perfect coherence across the measured frequency spectrum at the contraction exit for probe separation distances less than 2 cm.

When the probes were located at $x/L = 0.75$, the coherence function of the acoustically excited T2 flow (radial separation distance of 3 cm) shows a region of low coherence from about 350 to 525 Hz. See Fig. 12. Probe separations of 1 and 2 cm produced essentially identical frequency regions of low coherence. This is the net result of the combination of acoustic wave interference (resulting from reflections from the contraction's geometric boundaries) and some acoustic/turbulence interaction that was detected at that specific location. Evidence suggesting that acoustic/turbulence interaction may be involved here is provided by a similar coherence plot for flow condition T1 shown in Fig. 13. If acoustic/turbulence interaction did not play an important role, we would not expect the frequency range where the low coherence was observed in T1 and T2 to differ significantly. However, for T1, the region of low coherence occurs at a different frequency range (i.e., higher, at approximately 800 Hz). Further research

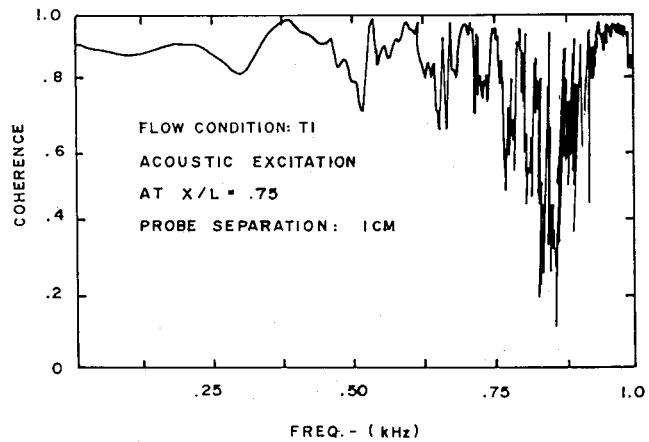

Fig. 13 Coherence function of streamwise velocity at $x/L = 0.75$ between two probes separated radially (1-cm probe separation: $r/R(x) = 0.17$) with acoustic excitation using flow condition T1.

is needed to provide a better understanding of this phenomenon.

Conclusions

The effect of imposing broadband acoustic excitation on a flow through an axisymmetric 14 : 1 contraction was investigated. For the moderately high contraction ratio used, acoustic excitation is very effective at augmenting the streamwise component of turbulence in the contracting region where the area is rapidly decreasing. With a 14 : 1 contraction, an acoustic excitation of 109-dB SPL can add over 20% to the apparent

streamwise component of turbulence energy in the central portion of the contracting section. Acoustic noise of this level is not uncommon in high-velocity airflows through regulating or control valves. An increase of the radial turbulence energy component was much smaller and amounted to less than 3% throughout most of the contracting section, except near the exit, where a more substantial increase was noticed.

The presence of significant randomly phased broadband acoustic energy in the flow tended to show a smaller variation of the u'/v' profile through a given contracting section. This characteristic would not be representative of flows that have similar u'/v' profiles but are not contaminated acoustically, because acoustically induced u'-like fluctuations are not randomly distributed in the radial direction.

Velocity spectra confirm that acoustic excitation increased the measured streamwise velocity fluctuations much more than the radial component. The acoustically excited u' spectra exhibits a minimum because of the interaction of turbulence and acoustic (i.e., pressure) reflections from the contraction boundary.

Almost perfect coherence in u' was observed between two radially separated probes when acoustic excitation was imposed. The coherence decreased when radial separation was increased. In the unexcited flow, coherence at the contraction exit is higher than at the inlet because residual blower-induced u'-like fluctuations are amplified by the contraction.

At $x/L = 0.75$, acoustically excited flow showed high coherence except for a small band of frequencies. This low-coherence frequency band was not a function of the probes' radial separation distance, but its location in the frequency spectrum and bandwidth seemed to depend on the upstream turbulence condition. It was suggested that this phenomenon is a net result of acoustic wave interference resulting from reflections from the contraction's geometric boundaries and some form of acoustic/turbulence interaction. Further research is necessary to provide a definitive explanation.

Acknowledgment

The authors would like to express their thanks to William Berent and his competent staff at the University's FEAS machine shop for modifying the flow facility to accommodate the present experiment and to Dr. Andrés Soom for loaning us the dual channel FFT analyzer and sound measuring equipment.

References

[1] Tsien, H.S., "On the Design of the Contraction Cone for a Wind Tunnel," *Journal of Aeronautical Sciences*, Vol. 10, 1943, pp. 68–70.

[2] Batchelor, G. and Shaw, F.S., "Consideration of Design of Wind Tunnel Contractions," *Australian Council for Aeronautics*, Rept. ACA–4, 1944.

[3] Smith, R.H. and Wang, C.T., "Contracting Cones Giving Uniform Throat Speeds," *Journal of Aeronautical Sciences*, Vol. 11, 1944, pp. 356–360.

[4] Thwaites, B., "On the Design of Contractions for Wind Tunnels," *Australian Research Council*, Report and Memorandum 2278, 1946.

[5] Jordinson, R., "Design of Wind Tunnel Contractions," *Aircraft Engineering*, Vol. 33, 1961, pp. 294–297.

[6] Cohen, M.J. and Ritchie, N.J.B., "Low-speed Three-dimensional Contraction Design," *Journal of the Royal Aeronautics Society*, Vol. 66, 1962, pp. 231–236.

[7] Bradshaw, P. and Pankhurst, R., "The Design of Low-Speed Wind Tunnels," *Progress in Aeronautical Sciences*, Vol. 5, 1964, pp. 1–69.

[8] Gay, B., Spettel, F., Jeandel, D., and Mathieu, J., "On the Design of the Contraction Section for a Wind Tunnel," *Journal of Applied Mechanics*, ASME, Vol. 40, 1973, pp. 309–310.

[9] Chmielewski, G.E., "Boundary-Layer Considerations in the Design of Aerodynamic Contractions," *Journal of Aircraft*, Vol. 11, Aug. 1974, pp. 435–438.

[10] Morel, T., "Comprehensive Design of Axisymmetric Wind Tunnel Contractions," *Journal of Fluids Engineering*, ASME, Vol. 97, 1975, pp. 225–233.

[11] Morel, T., "Design of Two-Dimensional Wind Tunnel Contractions," *Journal of Fluids Engineering*, ASME, Vol. 99, 1977, pp. 371–378.

[12] Nagib, H.M., Marion, A., and Tan-atichat, J., "On the Design of Contractions and Settling Chambers for Optimal Turbulence Manipulation in Wind Tunnels," AIAA Paper 84-0536, 1984.

[13] Comte-Bellot, G. and Corrsin, S., "The Use of a Contraction to Improve the Isotropy of Grid-Generated Turbulence," *Journal of Fluid Mechanics*, Vol. 25, 1966, pp. 657–682.

[14] Uberoi, M.S. and Wallis, S., "Small Axisymmetric Contraction of Grid Turbulence," *Journal of Fluid Mechanics*, Vol. 24, 1966, pp. 539–543.

[15] Uberoi, M.S., "Effect of Wind-Tunnel Contraction on Free-Stream Turbulence," *Journal of Aeronautical Sciences*, Vol. 23, 1956, pp. 754–764.

[16] Hussain, A.K.M.F. and Ramjee, V., "Effects of the Axisymmetric Contraction Shape on Incompressible Turbulent Flow," ASME Paper 75-FE-13, Fluids Engineering Conference, Minneapolis, MN, 1975.

[17] Ramjee, V. and Hussain, A.K.M.F., "Influence of the Axisymmetric Contraction Ratio on Free-Stream Turbulence," *Journal of Fluids Engineering*, ASME, Vol. 98, 1976, pp. 506–515.

[18] Tan-atichat, J., "Effects of Axisymmetric Contractions on Turbulence of Various Scales," Ph.D. Thesis, Illinois Institute of Technology, Chicago, 1980 (also available as NASA Contractor Rept. 165136).

[19] Loehrke, R.I. and Nagib, H.M., "Experiments on Management of Free-Stream Turbulence," AGARD Rept. 598, NATO, Neuilly Sur Seine, France, 1972.

[20] Loehrke, R.I. and Nagib, H.M., "Control of Free Stream Turbulence by Means of Honeycombs: A Balance Between Suppression and Generation," *Journal of Fluids Engineering*, ASME, Vol. 98, 1976, p. 342.

[21] Klein, A. and Ramjee, V., "Effects of Contraction Geometry on Non-Isotropic Free-Stream Turbulence," *Aeronautical Quarterly*, Vol. 24, 1973, pp. 34–38.

[22] Bennett, J.C. and Corrsin, S., "Small Reynolds Number Nearly Isotropic Turbulence in a Straight Duct and a Contraction," *Physics of Fluids*, Vol. 21, 1978, pp. 2129–2140.

[23] Goldstein, M.E. and Durbin, P., "The Effect of Finite Turbulence Spatial Scale on the Amplification of Turbulence by a Contracting Stream," *Journal of Fluid Mechanics*, Vol. 98, 1980, pp. 473–508.

[24] Tsugé, S., "Effects of Flow Contraction on Evolution of Turbulence," *Physics of Fluids*, Vol. 27, 1984, pp. 1948–1956.

[25] Kadman, Y. and Hayden, R.E., "Factors in the Design and Performance of Free-Jet Acoustic Wind Tunnels," AIAA Paper 75-531, 1975.

[26] *Aeroacoustics: Jet and Combustion Noise; Duct Acoustics, Progress in Astronautics and Aeronautics*, edited by H.T. Nagamatsu, AIAA, New York, Vol. 37, 1975.

[27] *Aeroacoustics: Fan Noise and Control; Duct Acoustics; Rotor Noise, Progress in Astronautics and Aeronautics*, edited by I.R. Schwartz, AIAA, New York, Vol. 44, 1976.

[28] Tan-atichat, J., Nagib, H.M., and Loehrke, R.I., "Interaction of Free-Stream Turbulence with Screens and Grids: A Balance Between Turbulence Scales," *Journal of Fluid Mechanics*, Vol. 114, 1982, pp. 501–528.

[29] Woo, T.K., "Design, Construction and Documentation of a Low Turbulence Hot-Wire Calibration Facility," M.S. Thesis, State Univ. of NY at Buffalo, 1982.

[30] Hultgren, L.S. and Chen, S.C., "Rapid Distortion of Small-scale Turbulence by an Axisymmetric Contraction," *Physics of Fluids*, Vol. 26, 1983, pp. 409–415.

[31] Batchelor, G. and Proudman, I., "The Effect of Rapid Distortion of a Fluid in Turbulent Motion," *Quarterly Journal of Mechanics and Applied Mathematics*, Vol. 7, 1954, pp. 83–103.

[32] Harandi, S., "Effects of Acoustic Excitation on Measured Turbulence Characteristics Through a Contraction," M.S. Thesis, State Univ. of NY at Buffalo, 1984.

[33] Huff, R.G., "The Effect of Acoustic Reflections on Combustor Noise Measurements," *Journal of Propulsion and Power*, Vol. 2, Jan./Feb., 1986, pp. 18–24.